Available online at www.sciencedirect.com

ScienceDirect

Advances in Space Research 55 (2015) 1630–1639

ADVANCES IN SPACE RESEARCH (a COSPAR publication)

www.elsevier.com/locate/asr

Correction's method of the electron density model in ionosphere by ray tracing techniques

Alessandro Settimi [a,*], Michael Pezzopane [a], Marco Pietrella [a], Carlo Scotto [a], Silvio Bianchi [b], James A. Baskaradas [c]

[a] *Istituto Nazionale di Geofisica e Vulcanologia (INGV), Sezione di Geomagnetismo, Aeronomia e Geofisica Ambientale (ROMA 2), Via di Vigna Murata 605, I-00143 Rome, Italy*

[b] *Università Sapienza, Dipartimento di Fisica, p.le Aldo Moro 2, I-00185 Rome, Italy*

[c] *School of Electrical & Electronics Engineering, Shanmugha Arts, Science, Technology & Research Academy (SASTRA) University, Tirumalaisamudram, Thanjavur, 613 401 Tamil Nadu, India*

Received 26 June 2014; received in revised form 11 December 2014; accepted 26 December 2014
Available online 5 January 2015

Abstract

When applying the ray tracing in ionospheric propagation, the electron density modelling is the main input of the algorithm, since phase refractive index strongly depends on it. Also the magnetic field and frequency collision modelling have their importance, the former as responsible for the azimuth angle deviation of the vertical plane containing the radio wave, the latter for the evaluation of the absorption of the wave. Anyway, the electron density distribution is strongly dominant when one wants to evaluate the group delay time characterizing the ionospheric propagation. From the group delay time, azimuth and elevation angles it is possible to determine the point of arrival of the radio wave when it reaches the Earth surface. Moreover, the procedure to establish the target (T) position is one of the essential steps in the Over The Horizon Radar (OTHR) techniques which require the correct knowledge of the electron density distribution. The group delay time generally gives rough information of the ground range, which depends on the exact path of the radio wave in the ionosphere. This paper focuses on the lead role that is played by the variation of the electron density grid into the ray tracing algorithm, which is correlated to the change of the electron content along the ionospheric ray path, for obtaining a ray tracing as much reliable as possible. In many cases of practical interest, the group delay time depends on the geometric length and the electron content of the ray path. The issue is faced theoretically, and a simple analytical relation, between the variation of the electron content along the path and the difference in time between the group delays, calculated and measured, both in the ionosphere and in the vacuum, is obtained and discussed. An example of how an oblique radio link can be improved by varying the electron density grid is also shown and discussed.

Keywords: Ionospheric ray tracing; Electron density model; Ray path correction; Electron content

1. Introduction

A ray tracing (RT) algorithm can be implemented by a computational program that traces the ionospheric path of the radio wave starting from initial conditions like coordinates, frequency, azimuth and elevation angles, and the physical models of the ionosphere (Haselgrove, 1955). A RT program computes the coordinates reached by the wave vector and its three components, represented in spherical coordinates, by integrating numerically a system of differential equations (Bianchi and Bianchi, 2009; Bianchi et al., 2009; Settimi et al., 2013b, 2014a; Settimi and Bianchi, 2014). Interesting quantities are also the ray

* Corresponding author. Tel.: +39 06 51860719; fax: +39 06 51860397.
E-mail addresses: alessandro.settimi@ingv.it (A. Settimi), michael.pezzopane@ingv.it (M. Pezzopane), marco.pietrella@ingv.it (M. Pietrella), carlo.scotto@ingv.it (C. Scotto), silvio.bianchi.phys@gmail.com (S. Bianchi), jamesbaskaradas@ece.sastra.edu (J.A. Baskaradas).

http://dx.doi.org/10.1016/j.asr.2014.12.035
0273-1177/

path and the apogee, which is the maximum elevation of the ray trajectory above the Earth surface. Moreover, other interesting values that a RT program provides as output are propagating quantities like the phase and group refractive index, the phase velocity, the absorption, and the Doppler frequency shift (Jones and Stephenson, 1975). Among these quantities, the group delay time t_c, calculated step by step along the ionospheric ray path, is particularly interesting for this paper. The reason is that the calculated group delay time t_c is easily comparable with the effective measured group delay time t_m in some technological applications, such as the Over The Horizon Radar (OTHR) oblique synchronized sounding or ionospheric backscatter (Davies, 1990). The calculated and measured group delay times are essential when one wants to check the performance of a RT program for given input parameters. The greater the difference in time between these two values, the weaker the performance of the RT program. However, we have to take into account that a RT algorithm is a deterministic computational process and an irrelevant error on t_c, due to the chosen integration step, is always present. The difference between the calculated and the measured group delay times t_c and t_m is strongly dependent on the difference between the electron density model and the real ionospheric conditions, especially in case of disturbances. For instance, when a RT program is applied to support an OTHR for surveillance of the target (T) localization, a challenging problem is posed; in fact, because of the electron density model approximation, the calculated and the measured group delay times t_c and t_m can differ significantly as well as the coordinate registration (CR) of the target (Davies, 1990). This means that, when illuminating a well known positioned target T (as for instance a coast profile or a geo-referenced radio transponder) by an OTHR, the CR depends significantly on the ionospheric electron density model given as input to the program. Whenever the target position is known, in order to check the validity of the results, which are strictly correlated to the correctness of the employed ionospheric electron density model, the calculated and the measured group delay times are compared. The possible difference in time between the two group delays can be ascribed only to the different electron densities encountered along the corresponding ionospheric ray paths. Since, in the ionized medium, the group delay time is proportional to both the ray path length and the electron density encountered along the same ray path (Budden, 1988), it is conceptually possible referring to a path inside a curved pipe of a 1 m^2 section characterized by a definite electron content (see Fig. 1). This paper represents a first simplified step in order to define a correction procedure for obtaining a reliable group delay time of the ionospheric ray path. In many cases of practical interest, the group delay time depends on the geometric length and the electron content of the ray path. The issue is faced theoretically, and a simple analytical relation, between the variation of the electron content along the path and the difference between t_c and t_m, both in the ionosphere and in the vacuum, is obtained and discussed. An example of how an oblique radio link can be improved by varying the electron density grid is also shown and discussed.

2. Ray path and ionospheric models

Ray tracing is a deterministic process of which the ionospheric ray path accuracy is arbitrarily chosen through the computational algorithm step (Haselgrove, 1955). Since the program provides the coordinates after each step, theoretically the process can be quantized into small steps. In doing so, the accuracy depends on the fineness of the step quantization, which can be pushed as far as it is desired. Practically, for high frequency (HF) RT programs, hundred–thousand steps are sufficient for the required accuracy. The major approximation is in the choice of the spatial extension of the cell where the electron density, the magnetic field and the collision frequency values are considered constant (Bianchi et al., 2010; Azzarone et al., 2012). For RT techniques, the collision frequency is nearly irrelevant because, concerning the HF propagation, it mainly affects the imaginary part of the phase refractive index, which is responsible for the wave absorption (Davies, 1990; Scotto and Settimi, 2013, 2014). On the contrary, the magnetic field affects both the field polarization and the ray trajectory, bending the wave vector as the radio wave penetrates the plasma.

In a collisionless magneto-plasma, the relation for the phase refractive index n, which takes into account the effects of the magnetic field, is given by Budden (1988):

$$n^2 = 1 - \frac{X}{1 - \frac{1}{2}\frac{Y_T^2}{(1-X)} \pm \sqrt{\frac{Y_T^4}{4(1-X)^2} + Y_L^2}}, \tag{1}$$

where: $X = \omega_p^2/\omega^2$ (ω being the angular frequency of the radio wave, $\omega_p = (Ne^2/m\varepsilon_0)^{1/2}$ the plasma frequency, N the electron density, m the electron mass, e the electron charge, and ε_0 the vacuum permittivity constant); $Y_T = Y\sin(\theta)$ and $Y_L = Y\cos(\theta)$ (θ being the angle between the wave vector and the direction of the Earth's magnetic field); and $Y = \omega_B/\omega$ ($\omega_B = Be/m$ being the gyro-frequency, and B the intensity of the Earth's magnetic field).

The presence of the magnetic field makes the plasma anisotropic (Davies, 1990). Even though it would be possible to estimate the ray path deviation due to the magnetic field contribution, nevertheless the phase refractive index employed in this paper is simplified by setting $B = 0$ in Eq. (1), as to obtain:

$$n^2 = 1 - X = 1 - \frac{\omega_p^2}{\omega^2}. \tag{2}$$

Apart from the constant values, the phase refractive index n represented by Eq. (2) depends on the angular frequency of the radio wave (hence on the corresponding frequency f), and the electron density N, of which the

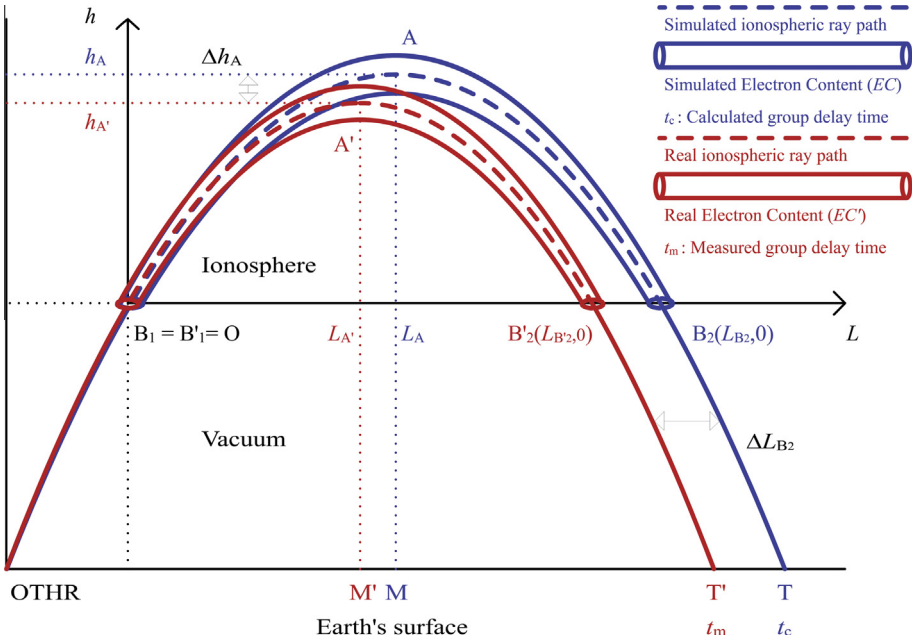

Fig. 1. A little change of electron content (*EC*) can imply great refractive effects: large variations for both the apogee (A) location and the path length of ionospheric ray tracing. The two ionospheric ray paths experience two different group delay times t_c and t_m, respectively the calculated and the measured group delay times.

corresponding model plays then a crucial role when applying RT algorithms.

3. Group delay time calculation

Neglecting the magnetic and collision effects, and employing only a discrete or analytic electron density model as input, a RT program provides as output the calculated group delay time t_c (Bianchi et al., 2011) depending on *EC*, which is evidently the simulated electron content along the ionospheric ray path, and other useful geometrical quantities. The calculated group delay time t_c can differ more or less significantly from the measured group delay time t_m (Settimi et al., 2013a, 2014b, in press) depending on the real electron content *EC'* along the ionospheric ray path. By means of t_m, it is possible to obtain the time difference $\Delta t = t_c - t_m$, relative to the simulated and real ray paths, which is function of $\Delta EC = EC - EC'$, i.e. the variation between the two electron contents along the simulated and real ray paths (see Fig. 1).

Considering the simulated ray path through the ionosphere between the transmitter (OTHR) and the receiver (target T), the relation for the calculated group delay time t_c can be derived as it follows (Bianchi, 1990):

$$t_c = \int_{OTHR}^{T} \frac{dl}{v_g(l)} = \frac{1}{c}\int_{OTHR}^{T} n_g(l)dl, \tag{3}$$

where c is the light velocity in vacuum, dl is the infinitesimal path length, v_g the group velocity, and n_g the group refractive index.

Since the phase refractive index n is commonly used in ionospheric propagation, the previous relation can be expressed in terms of n instead of n_g as:

$$t_c = \frac{1}{c}\int_{OTHR}^{T} \frac{dl}{n(l)} = \frac{1}{c}\int_{OTHR}^{T} \frac{dl}{\sqrt{1-\frac{\omega_p^2(l)}{\omega^2}}}. \tag{4}$$

For those radio waves propagating scarcely into the ionosphere, which is penetrated in correspondence to an oblique incidence, i.e. with low elevation angles, an approximate refractive index can hold throughout the HF band, i.e. 3–30 MHz. Indeed, under these operative conditions, the phase and group refractive indices can be approximated to the first-order Taylor's series expansion, and the square root into Eq. (4) becomes (Bianchi, 1990):

$$t_c \cong \frac{1}{c}\int_{OTHR}^{T}\left[1+\frac{\omega_p^2(l)}{2\omega^2}\right]dl. \tag{5}$$

Fig. 2 shows that the approximation made in Eq. (5) is acceptable when performing oblique radio links characterized by a low elevation angle; the ionospheric ray paths simulated by using Eqs. (4) and (5) are in fact in this case very similar.

Substituting in Eq. (5) the plasma frequency expression $\omega_p = (Ne^2/m\varepsilon_0)^{1/2}$, it results:

$$t_c \cong \frac{l_0}{c} + \frac{e^2}{2cm\varepsilon_0}\frac{1}{\omega^2}\int_{OTHR}^{T} N(l)dl, \tag{6}$$

where: l_0 is the length of ionospheric ray path from OTHR to T, $N(l)$ is the electron density along the ray path, and the integral of $N(l)\cdot dl$ along the same path is the electron content *EC* along a tube of a 1 m^2 section, corresponding to the path l_0.

In a perfect vertical propagation, the quantity $\int_{OTHR}^{T} N(l)dl$ of Eq. (6) represents the total electron content (TEC) (Bianchi, 1990). In many cases of practical interest, as proved by Eq. (6),

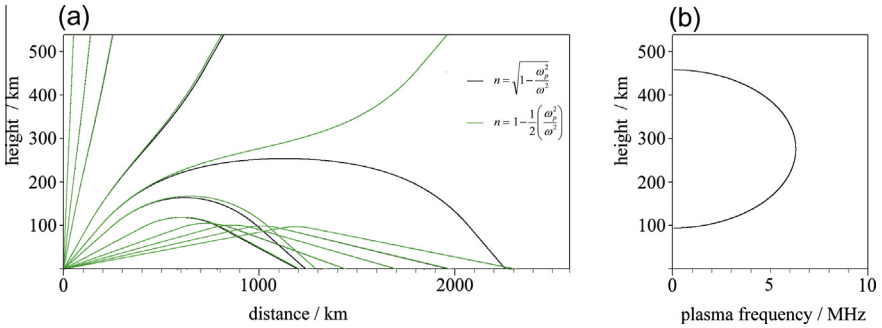

Fig. 2. (a) The ionospheric ray paths associated with a high frequency (HF) signal emitted from a transmitter (OTHR) at different elevation angles for a radio wave of frequency $f = 13.4$ MHz. The ray paths are computed with the exact and first-order Taylor's series expansion of the phase refractive index n. (b) The corresponding plasma frequency profile $f_p(h)$ of parabolic shape, with maximum $f_p^{(max)} = 6.784$ MHz at a height of 277 km, assuming $f_p(h) = 0$ MHz under 95 km and above 459 km.

two terms contribute to the calculated group delay time t_c: the term $t_{c0} = l_0/c$, which is the group delay time of the radio wave as calculated in vacuum, and the term proportional to $\int_{OTHR}^{T} N(l)\mathrm{d}l$, which is the extra group delay time suffered by the wave, depending on the electron content EC simulated along the ionospheric ray path and, in this case, due to the simulated electron density model.

Substituting the angular frequency ω with the frequency f expressed in MHz, Eq. (6) can be recast as:

$$t_c \cong t_{c0} + \frac{k}{f^2} EC, \tag{7}$$

where $k = (e^2/8\pi^2 cm\varepsilon_0)$ is a constant value equal to 1.34×10^{-19} [m^2 s^{-1}].

A similar relation can be written for the measured group delay time t_m:

$$t_m \cong t_{m0} + \frac{k}{f^2} EC', \tag{8}$$

where the first term t_{m0} is the group delay time of the radio wave as measured in vacuum, and the second term, analogously to Eq. (7), is the extra group delay time suffered by the wave, depending on the real electron content EC' along the ionospheric ray path and, in this case, due to the real electron density.

The time difference Δt between the group delays t_c and t_m can be written as:

$$\Delta t = t_c - t_m \cong t_{c0} - t_{m0} + \frac{k}{f^2}(EC - EC'), \tag{9}$$

or in a more compact form:

$$\Delta t \cong \Delta t_0 + \frac{k}{f^2}\Delta EC. \tag{10}$$

Eq. (10) quantifies the sum of the two contributions Δt_0 and $(k/f^2)\Delta EC$ as the time difference between the calculated and measured group delays Δt. A first order approximation of Eq. (10) can be applied when ΔEC is negligible, and Δt is in this case primarily imputable to Δt_0.

4. Correction of the electron density model

Throughout the HF band (3–30 MHz), the contribution of the second term in Eq. (10), considering an oblique incidence (low elevation angles), is generally less significant than the first term, though a slight variation ΔEC of electron content may modify significantly the ionospheric ray path and consequently the time difference Δt_0 between the group delays in vacuum. However, such a condition is quite common when the frequency f is below the plasma frequency f_p and the radio wave is reflected beneath the electron density maximum (Davies, 1990).

Neglecting the variation ΔEC of electron content, it follows that, as a first step, the time difference Δt between the group delays in ionosphere can be approximated to the time difference Δt_0 between the group delays in vacuum:

$$\Delta EC \to 0 \Rightarrow \Delta t \approx \Delta t_0. \tag{11}$$

With reference to Fig. 1, in blue and red colours are respectively represented the simulated and the real ray paths. The part inside the ionosphere is highlighted both by the dashed part of the curve and by the presence along the same ray path of the electron content tube. The points B_1, B_1' and B_2, B_2' draw the bottom of the ionosphere for both the radio waves. Indeed, the RT program, by computing the ray path in ionospheric plasma, produces as outputs respectively the points where the waves penetrate the plasma and the points where the waves come out the plasma, after passing across the related apogees A and A′, which give useful information concerning the plasma thickness penetrated by the waves. It is worth noting that the scenario shown in Fig. 1 is thought for a transmission frequency which is lower than the maximum usable frequency (MUF). In order to analyze in depth, the ionospheric ray path of interest is the path between $B_1(\equiv B_1')$ and B_2 (or B_2'), passing across the apogee A (or A′), by employing the simulated (or real) electron density model. Once fixed as origin the point $B_1 \equiv B_1' \equiv O(L_{B_1} = L_{B_1'} = 0, h_{B_1} = h_{B_1'} = 0)$, where the radio wave penetrates the ionosphere (clearly coincident for the simulated and

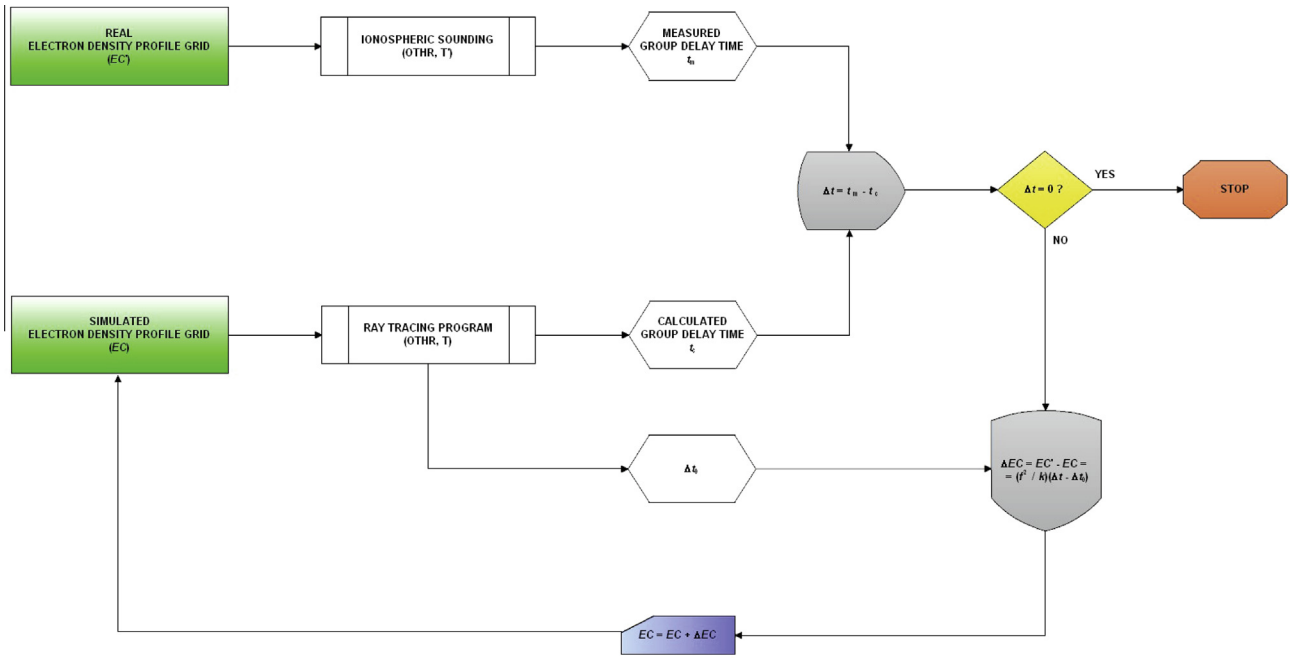

Fig. 3. Logic flowchart of an algorithm for the correction's method of the electron density model in ionosphere by ray tracing techniques.

real ray paths), further elements for evaluating Eq. (11) can be provided by a comparison between the pair of points $B_2(L_{B_2}, h_{B_2} = 0)$ and $B_2'(L_{B_2'} = L_{B_2} - \Delta L_{B_2}, h_{B_2'} = h_{B_2} = 0)$, where the wave comes out the ionosphere, and the pair of points $A(L_A = L_{B_2}/2, h_A)$ and $A'(L_{A'} = (L_{B_2} - \Delta L_{B_2})/2$, $h_{A'} = h_A - \Delta h_A)$, where the wave reaches the apogee (generally different for the two ionospheric ray paths). Hence, the time difference between the group delays $\Delta t \approx \Delta t_0$ (in vacuum), implies a length difference between the two ray paths equal to $c{\cdot}\Delta t_0$ (approximately). Assuming that both the simulated and real ray paths can be modelled by parabolic curves, if the two paths differ just a bit, i.e. $\Delta L_{B_2} \ll L_{B_2}$, $\Delta h_A \ll h_A$, once neglected the second-order infinitesimals, i.e. $\Delta L_{B_2} \cdot \Delta h_A \to 0$, then the time difference Δt_0 between the group delays in vacuum can be calculated approximately as [Appendix A]:

$$c\Delta t_0 \cong \frac{1}{8h_A^2}\left\{4L_{B_2}h_A\sqrt{1+16\left(\frac{h_A}{L_{B_2}}\right)^2}\,\Delta h_A + L_{B_2}(2h_A\Delta L_{B_2} - L_{B_2}\Delta h_A)\ln\left[4\frac{h_A}{L_{B_2}} + \sqrt{1+16\left(\frac{h_A}{L_{B_2}}\right)^2}\,\right]\right\} \tag{12}$$

Eq. (12) implies two simplified operative conditions: (1) as a first step, the simulated ray path, as well as the real ray path, can be approximately modelled by parabolic curves neglecting the variation of electron content ($\Delta EC \to 0$); (2) the distance Δh_A between the heights of the two apogees A and A′, as well as the distance ΔL_{B_2} between the ground ranges of the two out-coming points B_2 and B_2', must be estimated insofar the time difference Δt between the calculated and measured group delays in ionosphere tends to the corresponding value Δt_0 in vacuum as much as possible ($\Delta t \approx \Delta t_0$), in order to satisfy Eq. (11).

In reality, as a second step, the real ray path cannot be approximately modelled by a parabolic curve what's more by neglecting the variation of electron content (i.e. meaning that ΔEC should be $\neq 0$), condition for which the time difference Δt between the group delays in ionosphere does not tend exactly to the corresponding value Δt_0 in vacuum (i.e. meaning that Δt should be $\neq \Delta t_0$). A RT program could compute more realistic ray paths, by running a simulated electron density model which is corrected by adding algebraically a variation ΔEC of electron content, proportional to the algebraic sum Δt–Δt_0 between the group delay time differences in ionosphere Δt and vacuum Δt_0. From Eq. (10), it follows that:

$$\Delta EC \simeq \frac{f^2}{k}(\Delta t - \Delta t_0). \tag{13}$$

Concerning Eq. (13), Δt_0 can be always estimated by Eq. (12); Δt can be also estimated because t_m is a measured value, and an initial approximated value of t_c can be easily calculated, for instance, by running an eikonal based RT program (Scotto and Settimi, 2014), which is computed for a simplified ionosphere consisting of a single parabolic layer (see Fig. 2). In this way, Eq. (13) produces as output a value of ΔEC along the ionospheric ray path, corresponding just to the potential variation of electron density, which is considered as the starting value to launch an iterative procedure finalized to obtain a value of t_c comparable to the value of t_m. Fig. 3 shows the logic flowchart of the algorithm for the correction's method of the electron density model in ionosphere by ray tracing techniques. This

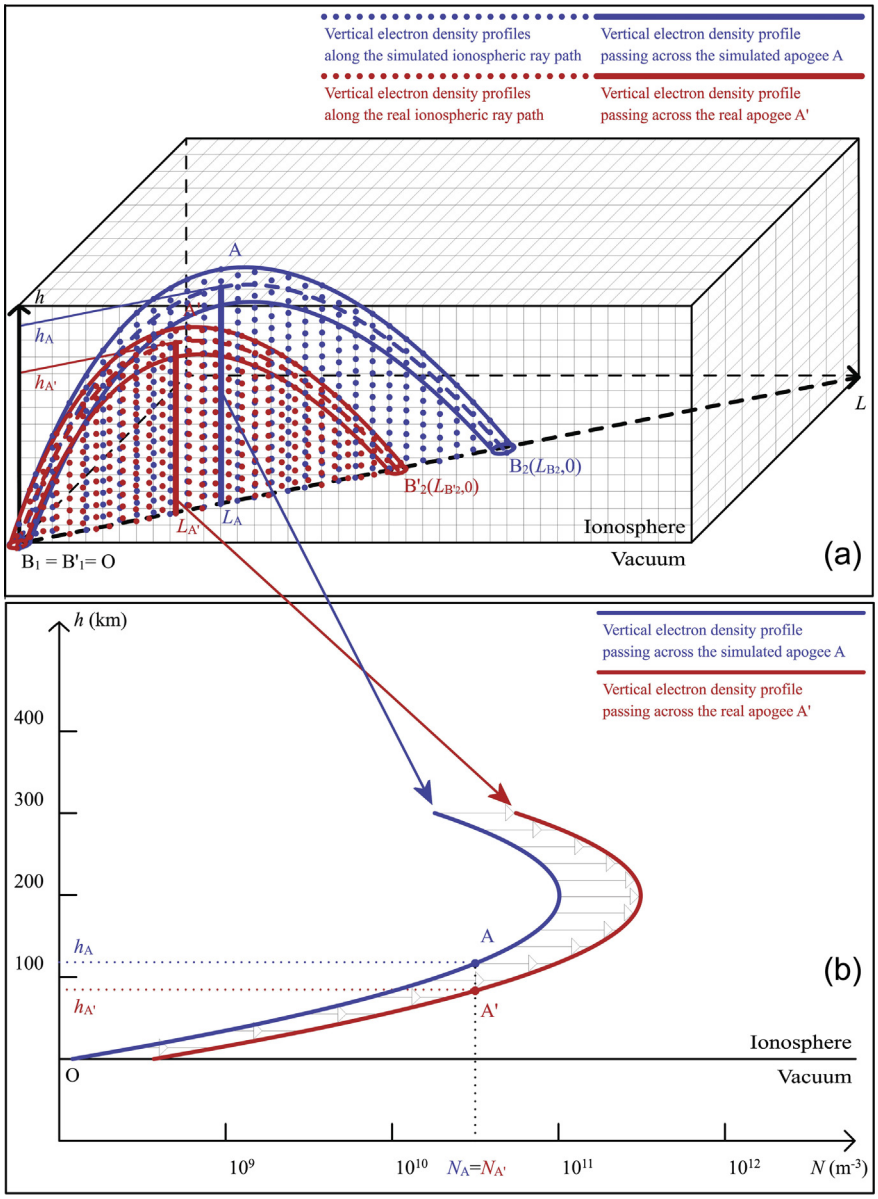

Fig. 4. (a) Vertical electron density profiles along the ionospheric ray path that have to be corrected compensating the time difference between the calculated and measured group delays in ionosphere. (b) The two vertical electron density profiles, plotted as a function of height, refer to the plumb lines passing across the simulated (A) or real (A′) apogees. The two vertical profiles correspond to the simulated (N) or real (N') electron densities over the simulated (M) or real (M′) midpoints between the transmitter (OTHR) and the simulated (T target) or real (T′ target) receiver of Fig. 1.

flowchart summarizes the steps of the iterative procedure that has been now described; it is worth highlighting that this procedure is characterized by a finite number of cycles, at the end of which the value ΔEC minimizing Δt is considered as the best representation of the ionospheric plasma, hence the best input for the RT program. Indeed, if the measured group delay time t_m is different from the calculated group delay time t_c, this can be ascribed to a non realistic representation of the electron density distribution provided by the model along the ray path, which has to be consequently and properly corrected to decrease as much as possible the time difference between the group delays, i.e. $\Delta t = t_c - t_m$.

In order to better define this concept, refer to Fig. 4 considering the vertical electron density profiles along the ionospheric path. The simulated ray path (with apogee A at height h_A from the bottom of ionosphere, corresponding to the midpoint M between the transmitter OTHR and the simulated target T) can be turned into the real ray path (with apogee A′ at height $h_{A'}$ from the bottom of ionosphere, corresponding to the midpoint M′ between the transmitter OTHR and the real target T′) (see Fig. 4a), just by correcting the simulated electron density profile $N(h)$, equal to N_A at height h_A, into the real electron density profile $N'(h)$, still equal to $N_{A'} = N_A$ but at different height $h_{A'} \neq h_A$ (see Fig. 4b). The two ray paths (passing across

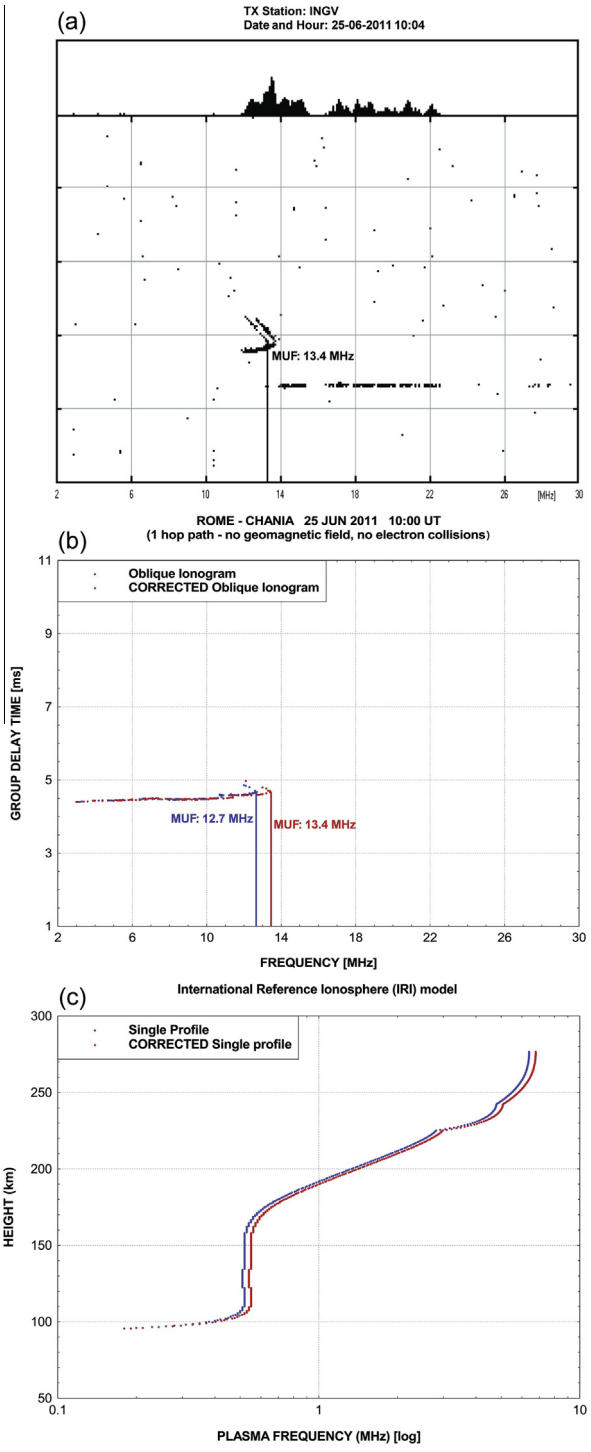

Fig. 5. (a) Oblique ionogram recorded on the 25 June 2011 at 10.00 UT along the Rome–Chania radio link, for which the maximum usable frequency MUF = 13.4 MHz value is highlighted. (b) Oblique ionogram synthesized by the IONORT-IRI system showing two ordinary traces corresponding to a plasma frequency profile $f_p(h)$ (trace in blue colour), with a MUF = 12.7 MHz (signed in blue colour), and to a corrected plasma frequency profile $f_p(h) + 0.06{\cdot}f_p(h)$ (trace in red), with a MUF = 13.4 MHz (signed in red). (c) The plasma frequency profile $f_p(h)$ (in blue) and the corrected plasma frequency profile $f_p(h) + 0.06{\cdot}f_p(h)$ (in red) used by IONORT to synthesize the traces shown in b). (For interpretation of the references to colour in this figure legend, the reader is referred to the web version of this article.)

the simulated and real apogees A and A′), are characterized by two different values of electron content, simulated EC and real EC', which allow to define the re-distribution function $\Delta EC = EC–EC'$, useful to correct the electron content profiles over the entire ionosphere. If the simulated apogee A is in a linear region of the electron density profile, a right correction can be adequately provided by linearly re-distributing ΔEC. Otherwise, exponential or parabolic rearrangement of ΔEC must be assumed. However, a preliminary phase of test has demonstrated that fine results can be obtained by adopting a linear re-distribution of the electron density along the whole profile.

Nonetheless, in this paper, the theoretical results shown by Eqs. (10) and (13) were not yet coded in a RT program that could process the value of ΔEC along the ionospheric ray path, which is considered as the starting value to launch an iterative procedure with the aim to reset the time difference between the group delays ($\Delta t \approx \Delta t_0 \approx 0$). At the present moment, a RT applicative software tool package, named IONORT, which was developed by Azzarone et al. (2012), has implemented just an iterative procedure by which the electron density profiles are corrected, thus simulating the re-distribution function ΔEC, in order to match the measured and calculated MUFs related to definite radio links.

With regard to this issue, let us consider a radio link, with one ionospheric reflection (1 hop path), between a transmitter (OTHR), located in Rome, Italy ($lat_1 = 41.89°$N, $lon_1 = 12.48°$E) and a receiver (target T), located in Chania, Crete ($lat_2 = 35.51°$N, $lon_2 = 24.02°$E). The International Reference Ionosphere (IRI)-2007 model (Bilitza and Reinisch, 2008) allows computing the electron density profile, on any date and time, relative to the midpoint M between OTHR and T, i.e. M = [$lat_M = (lat_1 + lat_2)/2 = 38.70°$N, $lon_M = (lon_1 + lon_2)/2 = 18.25°$E]. Let use IONORT program, simulating a ray tracing of radio waves in the ionospheric medium, in conjunction with IRI-2007 model, in order to synthesize oblique ionograms of the radio link between OTHR and T. Note that a stationary ionosphere is assumed to be approximately valid throughout the region of the performed radio link. Indeed, suitable operative conditions must hold to apply the theorems of Breit and Tuve (1926), Martyn (1935) and Davies (1990). Accordingly, the real oblique sounding between the stations of OTHR and T can be turned into a virtual oblique sounding, which oblique sounding, in turn, is reduced to a virtual vertical sounding along the vertical line of the midpoint M. More precisely, the Breit & Tuve's and Martyn's theorems should be applied during hours of the day in which the ionospheric medium is characterized by small horizontal gradients, when the azimuth angle of transmission is assumed to be a constant along the great circle path (Settimi et al., 2013a, 2014b, in press). By the way, IONORT program can be ideally used for a flat layering ionosphere, without any horizontal gradient, so characterized by an electron density profile $N(h)$ dependent

only on the altitude h. At the limit, a single profile for $N(h)$ recurs throughout the latitude and longitude grid of points involved in the ray tracing computation (Scotto and Settimi, 2014).

In Fig. 5, a comparison between the ordinary trace of the oblique ionogram recorded over the Rome–Chania radio link on 25 June 2011 at 10:00 UT and the corresponding ionogram synthesized by the IONORT-IRI system is shown. The synthesized oblique ionogram, with 1 hop path, is computed without taking into account both the geomagnetic field and electron collisions. The IRI-2007 profile, relative to the midpoint M between OTHR and T, is represented by a single profile of plasma frequency $f_p(h)$ as a function of height h. The IRI-2007 profile is replicated throughout the region involved in the performed radio link, and it is recursively corrected after 6 iterations, each adding a basic step equal to $\Delta f_p(h) = 0.01 \cdot f_p(h)$, so that the calculated MUF_c coincides with the measured MUF_m stopping to a final linear shift equal to $6 \cdot \Delta f_p(h)$.

5. Conclusions

A prior determination of the ionospheric ray path in applications involving radio wave propagation, such as the Over The Horizon Radar (OTHR) surveillance and tracking, remote sensing measurements through electromagnetic waves and precise oblique sounding, needs a ray tracing (RT) algorithm to be used. Being a RT program a deterministic computational procedure whose accuracy depends on the integration step, the only source of error is mainly referable to the electron density model representing the input parameter. Because of long and short terms variability, electron density distribution constitutes the sensitive point in this technique. Rarely operators can provide an electron density model with the required accuracy, actually very often the discordance from the real representation of the ionospheric medium is significant and the model must be corrected. This paper demonstrated theoretically that, after the only possible measurement, which is the measured group delay time t_m, the correction can be performed: indeed, this quantity, compared with the calculated group delay time t_c, allows to calculate the time difference Δt between the group delays in ionosphere. This paper represented a first simplified step in order to define a correction procedure for obtaining a reliable group delay time of the ionospheric ray path. In many cases of practical interest, the group delay time depends on the geometric length and the electron content of the ray path. The issue was faced theoretically, and a simple analytical relation, between the variation of the electron content along the path and the difference between t_c and t_m, both in the ionosphere and in the vacuum, was obtained and discussed. An example of how an oblique radio link can be improved by varying the electron density grid was also shown and discussed. The practical application of our proposed correction's method for the electron density model in ionosphere by ray tracing techniques, and its operational use, will be our goal in a forthcoming paper.

Appendix A

Referring to the plane frame Lh, once fixed as its origin the point $B_1 \equiv B_1' \equiv O\left(L_{B_1} = L_{B_1'} = 0, h_{B_1} = h_{B_1'} = 0\right)$ (see Fig. 1), the parabola that passes through the origin B_1 and the pair of points (blue colour)

$$B_2(L_{B_2}, h_{B_2} = 0), \quad A\left(L_A = \frac{L_{B_2}}{2}, h_A\right), \tag{A.1}$$

satisfies the equation:

$$h - h_A = -4\frac{h_A}{L_{B_2}^2}\left(L - \frac{L_{B_2}}{2}\right)^2. \tag{A.2}$$

The length of parabola (A.2) is calculated by the line integral along curvilinear abscissa:

$$\begin{aligned}\Gamma_{B_1-A-B_2} &= \int_{B_1}^{B_2} ds = \int_0^{L_{B_2}} dL\sqrt{1 + \left(\frac{dh}{dL}\right)^2} \\ &= \int_0^{L_{B_2}} dL\sqrt{1 + 64\left(\frac{h_A}{L_{B_2}^2}\right)^2\left(L - \frac{L_{B_2}}{2}\right)^2} \\ &= \frac{1}{2}L_{B_2}\sqrt{1 + 16\left(\frac{h_A}{L_{B_2}}\right)^2} + \frac{1}{8}\frac{L_{B_2}^2}{h_A} \\ &\quad \times \ln\left[4\frac{h_A}{L_{B_2}} + \sqrt{1 + 16\left(\frac{h_A}{L_{B_2}}\right)^2}\right]\end{aligned} \tag{A.3}$$

Instead, the parabola that passes through the origin B_1 and the pair of points (red colour)

$$\begin{aligned}&B_2'\left(L_{B_2'} = L_{B_2} - \Delta L_{B_2}, h_{B_2'} = h_{B_2} = 0\right), \\ &A'\left(L_{A'} = \frac{L_{B_2} - \Delta L_{B_2}}{2}, h_{A'} = h_A - \Delta h_A\right),\end{aligned} \tag{A.4}$$

satisfies the equation:

$$h - (h_A - \Delta h_A) = -4\frac{h_A - \Delta h_A}{(L_{B_2} - \Delta L_{B_2})^2}\left(L - \frac{L_{B_2} - \Delta L_{B_2}}{2}\right)^2. \tag{A.5}$$

The length of parabola (A.5) is calculated by the line integral along curvilinear abscissa:

$$\Gamma_{B_1-A'-B'_2} = \Gamma_{B_1-A-B_2}|_{L_{B_2}\to L_{B'_2}=L_{B_2}-\Delta L_{B_2}, h_A\to h_{A'}=h_A-\Delta h_A}$$
$$= \frac{1}{2}(L_{B_2}-\Delta L_{B_2})\sqrt{1+16\left(\frac{h_A-\Delta h_A}{L_{B_2}-\Delta L_{B_2}}\right)^2} + \frac{1}{8}\frac{(L_{B_2}-\Delta L_{B_2})^2}{h_A-\Delta h_A} \times \ln\left[4\frac{h_A-\Delta h_A}{L_{B_2}-\Delta L_{B_2}}+\sqrt{1+16\left(\frac{h_A-\Delta h_A}{L_{B_2}-\Delta L_{B_2}}\right)^2}\right], \quad (A.6)$$

If the two parabolas differ just a bit, i.e.

$$\Delta L_{B_2} \ll L_{B_2}, \quad \Delta h_A \ll h_A, \quad (A.7)$$

then Eq. (A.6) can be approximated to its Taylor's series expansion at the first order in ΔL_{B_2} and Δh_A , as it follows:

$$\Gamma_{B_1-A'-B'_2} \cong \frac{1}{8}\frac{L_{B_2}}{h_A^2}\sqrt{1+16\left(\frac{h_A}{L_{B_2}}\right)^2}\left[\frac{1}{2}\frac{h_A-\Delta h_A}{h_A}+\frac{\frac{\Delta L_{B_2}}{L_{B_2}}\frac{\Delta h_A}{h_A}}{1+16\left(\frac{h_A}{L_{B_2}}\right)^2}\right] + \frac{1}{8}\frac{L_{B_2}}{h_A^2}(L_{B_2}-2\Delta L_{B_2})(h_A+\Delta h_A)\ln\left[4\frac{h_A}{L_{B_2}}+\sqrt{1+16\left(\frac{h_A}{L_{B_2}}\right)^2}\right]. \quad (A.8)$$

The length difference between parabolas (A.2) and (A.5) is calculated subtracting Eqs. (A.3) and (A.8) member by member:

$$\Delta\Gamma = \Gamma_{B_1-A-B_2} - \Gamma_{B_1-A'-B'_2} \cong \frac{1}{2}\frac{L_{B_2}}{h_A}\sqrt{1+16\left(\frac{h_A}{L_{B_2}}\right)^2}\left[1-\frac{2\frac{\Delta L_{B_2}}{L_{B_2}}}{1+16\left(\frac{h_A}{L_{B_2}}\right)^2}\right]\Delta h_A + \frac{1}{8}\frac{L_{B_2}}{h_A^2}[2h_A\Delta L_{B_2}-(L_{B_2}-2\Delta L_{B_2})\Delta h_A]\ln\left[4\frac{h_A}{L_{B_2}}+\sqrt{1+16\left(\frac{h_A}{L_{B_2}}\right)^2}\right]. \quad (A.9)$$

Neglecting second-order infinitesimals, i.e.

$$\Delta L_{B_2}\cdot\Delta h_A \to 0, \quad (A.10)$$

Eq. (A.9) can be simplified as it follows:

$$\Delta\Gamma \simeq \frac{1}{8h_A^2}\left\{4L_{B_2}h_A\sqrt{1+16\left(\frac{h_A}{L_{B_2}}\right)^2}\Delta h_A + L_{B_2}(2h_A\Delta L_{B_2}-L_{B_2}\Delta h_A)\ln\left[4\frac{h_A}{L_{B_2}}+\sqrt{1+16\left(\frac{h_A}{L_{B_2}}\right)^2}\right]\right\}. \quad (A.11)$$

The length difference between parabolas (A.5) and (A.2) is reset to zero, i.e.

$$\Delta\Gamma = 0, \quad (A.12)$$

under the following condition:

$$\Delta L_{B_2} \simeq \Delta h_A\left\{\frac{1}{2}\frac{L_{B_2}}{h_A}-2\frac{\sqrt{1+16\left(\frac{h_A}{L_{B_2}}\right)^2}}{\ln\left[4\frac{h_A}{L_{B_2}}+\sqrt{1+16\left(\frac{h_A}{L_{B_2}}\right)^2}\right]}\right\}. \quad (A.13)$$

In the limit case $h_A \ll L_{B_2}$, Eq. (A.13) can be reduced as:

$$\Delta L_{B_2} \approx \Delta h_A\left[\frac{1}{2}\frac{L_{B_2}}{h_A}-\frac{2}{\ln\left(1+4\frac{h_A}{L_{B_2}}\right)}\right], \quad (A.14)$$

and, in the opposite case $h_A > L_{B_2}$, as:

$$\Delta L_{B_2} \approx \Delta h_A\left[\frac{1}{2}\frac{L_{B_2}}{h_A}-\frac{8\frac{h_A}{L_{B_2}}}{\ln\left(8\frac{h_A}{L_{B_2}}\right)}\right]. \quad (A.15)$$

References

Azzarone, A., Bianchi, C., Pezzopane, M., Pietrella, M., Scotto, C., Settimi, A., 2012. IONORT: a Windows software tool to calculate the HF ray tracing in the ionosphere. Comput. Geosci. UK 42, 57–63. http://dx.doi.org/10.1016/j.cageo.2012.02.008.

Bianchi, C., 1990. Note sulle interazioni delle onde elettromagnetiche con il plasma ionosferico, Istituto Nazionale di Geofisica, U. O. Aeronomia, Rome, Italy, 149 pp. [in Italian].

Bianchi, C., Bianchi, S., 2009. Problema generale del ray-tracing nella propagazione ionosferica – formulazione della "ray theory" e metodo del ray tracing, Rapporti Tecnici INGV, 104, 26 pp. [in Italian].

Bianchi, S., Sciacca, U., Settimi, A., 2009. Teoria della propagazione radio in mezzi disomogenei, Quaderni di Geofisica, 75, 14 pp. [in Italian].

Bianchi, C., Settimi, A., Azzarone, A., 2010. IONORT: IONOsphere Ray-Tracing. Programma di ray-tracing nel magnetoplasma ionosferico, Rapporti Tecnici INGV, 161, 20 pp. [in Italian].

Bianchi, C., Settimi, A., Scotto, C., Azzarone, A., Lozito, A., 2011. A method to test HF ray tracing algorithm in the ionosphere by means of the virtual time delay. Adv. Space Res. 48 (10), 1600–1605. http://dx.doi.org/10.1016/j.asr.2011.07.020.

Bilitza, D., Reinisch, B.W., 2008. International reference ionosphere 2007: improvements and new parameters. Adv. Space Res. 42 (4), 599–609. http://dx.doi.org/10.1016/j.asr.2007.07.048.

Breit, G., Tuve, M.A., 1926. A test of the existence of the conducting layer. Phys. Rev. 28 (3), 554–575. http://dx.doi.org/10.1103/PhysRev.28.554.

Budden, K.G., 1988. The Propagation of Radio Waves: The Theory of Radio Waves of Low Power in the Ionosphere and Magnetosphere. Cambridge University Press, Cambridge, UK, pp. 688.

Davies, K., 1990. Ionospheric Radio, Peter Peregrinus Ltd. (ed.) on behalf of the Institution of Electrical Engineers (IET), London, UK, 508 pp.

Haselgrove, J., 1955. Ray theory and a new method of ray tracing. In: Conference on the Physics of the Ionosphere, Proceedings of Physics Society London, vol. 23, pp. 355–364.

Jones, R.M., Stephenson, J.J., 1975. A versatile three-dimensional ray tracing computer program for radio waves in the ionosphere, OT Report, 75–76, US Department of Commerce, Office of Telecommunication, US Government Printing Office, Washington, USA, 185 pp.

Martyn, D.F., 1935. The propagation of medium radio waves in the ionosphere. Proc. Phys. Soc. 47 (2), 323–339. http://dx.doi.org/10.1088/0959-5309/47/2/311.

Scotto, C., Settimi, A., 2013. The effect of collisions in ionogram inversion. Adv. Space Res. 51 (5), 697–701. http://dx.doi.org/10.1016/j.asr.2012.09.033.

Scotto, C., Settimi, A., 2014. The calculation of ionospheric absorption with modern computers. Adv. Space Res. 54 (8), 1642–1650. http://dx.doi.org/10.1016/j.asr.2014.06.017.

Settimi, A., Bianchi, S., 2014. Ray theory formulation and ray tracing method, Application in ionospheric propagation. Quaderni di Geofisica 121, 21 pp.

Settimi, A., Pezzopane, M., Pietrella, M., Bianchi, C., Scotto, C., Zuccheretti, E., Makris, J., 2013a. Testing the IONORT-ISP system: a comparison between synthesized and measured oblique ionograms. Radio Sci. 48 (2), 167–179. http://dx.doi.org/10.1002/rds.20018.

Settimi, A., Sciacca, U., Bianchi, C., 2013b. Scientific review on the complex Eikonal, and research perspectives on the ionospheric ray-tracing and absorption. Quaderni di Geofisica 112, 29 pp.

Settimi, A., Ippolito, A., Cesaroni, C., Scotto, C., 2014a. Scientific review on the ionospheric absorption and research perspectives of a complex Eikonal model for one-layer ionosphere. Int. J. Geophys. 2014. http://dx.doi.org/10.1155/2014/657434. Article ID 657434, 14 pp.

Settimi, A., Pietrella, M., Pezzopane, M., Zolesi, B., Bianchi, C., Scotto, C., 2014b. The COMPLEIK subroutine of the IONORT-ISP system for calculating the non-deviative absorption: a comparison with the ICEPAC formula. Adv. Space Res. 53 (2), 201–218. http://dx.doi.org/10.1016/j.asr.2013.10.035.

Settimi A., Pietrella M., Pezzopane M., Bianchi C., in press. The IONORT-ISP-WC system: inclusion of an electron collision frequency model for the D-layer, *Adv. Space Res.* http://dx.doi.org/10.1016/j.asr.2014.07.040.